Functional Barriers in PET Recycled Bottles. Part II. Diffusion of Pollutants During Processing

P. Y. Pennarun, Y. Ngono, P. Dole, A. Feigenbaum

INRA (ADEME, ECO EMBALLAGES), CPCB Moulin de la Housse, 51687 Reims Cedex 2, France

Received 30 June 2003; accepted 22 October 2003

ABSTRACT: Recycled plastics may be polluted by various chemicals available to consumers. When such materials are used to manufacture packaging materials intended to be in direct contact with food, these pollutants may migrate into food. The use of multilayer structures with a virgin polymer layer as a functional barrier may prevent such migration. This work deals with the possible diffusion of pollutants into and through the virgin layer during processing at high temperatures. A test is designed to measure diffusion coefficients in elastomeric and glassy polymers, in their molten state; 2.5-dimethoxyacetophenone was used as a surrogate pollutant, and its concentration profiles are monitored by UV microscopy. Based on diffusion coefficients and on activation energies, glassy polymers appear to be much better barriers than polyolefins, even in their molten state. We then focus on poly(ethylene terephthalate) (PET) bottle preforms, processed by injection molding. In a first approach, a worst case situation was simulated by numerical analysis, using both overestimated diffusion coefficient values and very low values of activation energy. It appears that migration into foodstuffs through functional barriers can only be observed with unrealistic high diffusion coefficients and low activation energies. These results were confirmed by experimental determination of the concentration gradients of model pollutants in multilayer structures. It appears that little diffusion occurs, despite at a very high temperature. The effects of temperature and thickness of the functional barrier are discussed. J Appl Polym Sci 92: 2859–2870, 2004

Key words: PET; diffusion; functional barrier; modeling; food packaging

INTRODUCTION

The possibility of recycling plastics into food-contact materials has been largely studied.[1,2] Many technologies are now available. However, because recovered plastics may be polluted by various chemicals, when food packaging materials are produced, each process must be carefully optimized in terms of plastics purification (removal of low-molecular chemical contaminants) for preventing the migration of the pollutants into food. A possible approach consists of making articles where the recycled plastic is incorporated into multilayer structures, and thus, separated from the food by a layer of new (virgin) polymer, which is then deemed to behave as a barrier layer (called functional barrier) to migration.

The functional barrier may play its role as long as it is not itself polluted by the contaminants, a situation which may already occur when the contaminated layer and the functional barrier are assembled at high temperature. There has been considerable work in literature focusing on migration from such multilayer structures, where the layer (called here inner layer) located beyond the food contact layer (the functional barrier) has been deliberately polluted with model contaminants (surrogates). Some authors have modeled the migration behavior from such structures, emphasizing that the governing factors are (1) the diffusion coefficient of the pollutant in migration conditions (at ambient temperature), and (2) the initial pollution of the barrier layer after its processing (e.g., coextrusion or coinjection). To simulate diffusion during processing, Piringer[3,4] uses a constant (and very high) diffusion coefficient, whereas Perou et al.[5,6] uses a diffusivity gradient, described by time- and space-dependent temperature gradients during processing. The problem is (1) to describe correctly the temperature gradient (i.e., to know all the details of the process conditions, particularly cooling conditions), and (2) to use correct values of diffusion constants.

The current article focused on diffusion between the different layers during poly(ethylene terephthalate) (PET) preform injection. The two following methods will be used to demonstrate that the diffusion during processing leads to a negligible pollution of the barrier: (1) numerical simulations, using diffusion coefficients at molten state, measured by UV microscopy; and (2) experimental concentration depth profiling from artificially polluted multilayer bottles. In addi-

Correspondence to: A. Feigenbaum.
Contract grant sponsor: ECO-EMBALLAGES.
Contract grant sponsor: ADEME.
Contract grant sponsor: Region Champagne-Ardenne.

Journal of Applied Polymer Science, Vol. 92, 2859–2870 (2004)

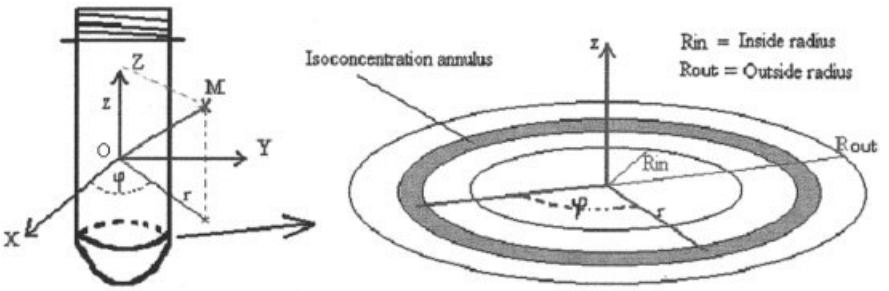

Figure 1 Representation of a preform: polar coordinates.

tion, a method is designed to determine diffusion coefficients in molten polymers.

NUMERICAL SIMULATION OF DIFFUSION IN PREFORMS DURING COINJECTION

Diffusion in a plane sheet

The mathematical treatment of diffusion kinetics of chemical substances and of heat is based on concentration or temperature gradients between two zones separated by a homogeneous medium. The flux of a chemical or temperature across a plane perpendicular to the diffusion direction is proportional to the concentration or to the temperature gradient. The mathematical treatment for concentration and temperature are the same.

These gradients follow the Fick's law for matter and the Fourier law for heat:

$$\text{Second Fick's law:} \quad \frac{\partial C}{\partial t} = \frac{\partial}{\partial x}\left(D\frac{\partial C}{\partial x}\right) \tag{1}$$

$$\text{Fourier's law:} \quad \rho C_p\left(\frac{\partial T}{\partial t}\right) = \frac{\partial}{\partial x}\left(\lambda\frac{\partial T}{\partial x}\right) \tag{2}$$

where C is the diffusant concentration, x is the thickness of the section considered, t is the time, D is the diffusion coefficient (diffusivity), T is the temperature (K), ρ is the material density, C_p is the heat capacity at a constant pressure, and λ is the thermal conductivity.

If ρC_p is constant, eq. (2) can be simplified by introducing α, the thermal diffusivity:

$$\frac{\partial C}{\partial t} = \frac{\partial}{\partial x}\left(\alpha\frac{\partial T}{\partial x}\right) \tag{3}$$

where $\alpha = \lambda/\rho C_p$. Mathematical resolution of these equations is quite difficult because the temperature and concentration dependence with x and t is not known. Numerical analysis is used, with Taylor developments[7,8]; the thickness is segmented into 100 elementary volumes.

Boundary conditions

A convection parameter, h_C, and the concentration in the external medium are introduced to take into account mass transfer at interface. The first Fick's law leads to

$$-D_{x=0}\left(\frac{\partial C}{\partial x}\right)_{x=0} = h_c(C_{x=0} - C_{\text{ext}}) \tag{4}$$

where h_C is a convection parameter at the surface in contact with the medium in contact, and C_{ext} is the concentration in this medium.

The same equation is obtained for heat diffusion (replacing C by T, D by α, and h_C by h_T).

Diffusion in a cylinder with symmetry axis (fig. 1)

Because the preform is a cylinder with thick walls, it can be assumed as an infinite cylinder, in the direction of symmetry axis OZ. As a result, eq. (1) can be written as:

$$\frac{\partial C}{\partial t} = \frac{\partial}{\partial r}\left(D\frac{\partial C}{\partial r}\right) + \frac{D}{r}\frac{\partial C}{\partial r} \tag{5}$$

where r is the radial distance perpendicular to the z-axis (Fig. 1).

Application to multilayer preform processing (fig. 2)

When preforms are manufactured, PET injection into the mold takes place in three steps. First, virgin PET is injected into the mold, the walls being efficiently cooled (a, b) (Fig. 2). Zones in contact with the mold begin immediately cooling (c). Temperature and viscosity gradients appear in the material.

In a second step, while the virgin PET is still molten in the middle of the mold (c), recycled PET is injected (d). Virgin molten PET is pushed and continues to fill the mold until it reaches the top of the mold. New virgin PET zones in contact with the mold are cooling

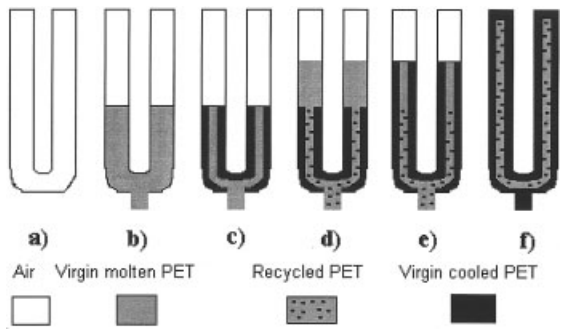

Figure 2 Different steps of multilayer preform injections. See text for a, b, c, d, e, and f states.

(e). [Pictures (d) and (e) represent continuous injection (the real situation is an average of each).]

Finally, virgin resin is injected to ensure filling of the mold and to compensate for thermal retraction of the preform (f).

The following experimental parameters, obtained from the manufacturer, are used for the modeling of the process. The inside and outside radiuses are 0.8895 and 1.3210 cm, respectively. Time 0 stands for the beginning of the injection. Virgin PET is injected up to $t = 4.3$ s. Recycled PET (25% of the preform) is injected for 1.5 s in the middle of the preform. Then, the preform is cooled.

Assumptions for heat transfer modeling

The mold (core and walls) is kept at constant temperature equal to 8°C (information given by the manufacturer).

Two cases of heat convection between PET and the mold wall are considered: $h_T = +\infty$ (perfect convection) and $h_T = 0.0074$ (typical value representing a poor convection), for a temperature of 110°C at the surface of PET, 30 s after injection (information given by manufacturer).

The PET does not crystallize, even for the lowest value of convection factor h_T.

The temperature at time $t = 0$ is homogeneous all over the preform and equal at 280°C.

Thermal diffusivity $\alpha(T)$ is linear in two different temperature intervals:[9]

$$\text{for } T>503\text{ K} \quad \alpha(T) = -0.02 \times 10^{-3} \times T + 11.46 \times 10^{-3} \tag{6}$$

$$\text{for } T<503\text{ K} \quad \alpha(T) = -4.565 \times 10^{-6} \times T + 3.546 \times 10^{-3}$$

where T is the temperature (K).

Assumptions on surrogate diffusion in PET

The diffusivity D follows an Arrhenius-type behavior: $D = D_0 \exp(-E_A/RT)$, where E_A is the activation energy of diffusion (J mol^{-1}), T is the temperature (K), R is the perfect gas constant (8.315 J mol^{-1} K^{-1}), and the preexponential factor D_0 is a constant (defined by the values of E_A and D at a reference temperature).

Surrogates (Table I) or pollutants are homoge-

TABLE I
Surrogates Used and Their Classification

Set	Surrogates	Properties	M (g/mol)	Solubility in water	Concentration (mg/kg impregnated PET bottle)
A	1,1,1-Trichloroethane	V, MP, BP = 75°C	M = 133	<1000 ppm (20°C)[10]	2690
A	Dimethyl sulfoxyde (DMSO)	NV, P, BP = 189°C	78	Very soluble[11]	1363
A	Methyl palmitate	NV, NP	270	Not soluble[11]	704
A	Benzophenone	NV, MP, BP = 305°C	182	<1000 ppm (20°C)[12]	2910
A	Phenylcyclohexane	NV, NP, BP = 240°C	160	Not soluble[11]	1285
A	Ethyl hydrocinnamate	MV, NP, BP = 247°C	178	Not soluble[11]	587
B	Phenol	NV, P, BP = 182°C	94	93 g/L (25°C)[10]	2616
B	2,6-Di-*tert*-butyl-4-methylphenol (BHT)	NV, MP, BP = 265°C	220	<0.01 g/L (20°C)[13]	872
B	Chlorobenzene	V, P, BP = 131°C	113	500 ppm (20°C)[10]	1324
B	2,5-Thiophenediylbis(5-*tert*-butyl-1,3-benzoxazole) (Uvitex)	Fluorescent dye	431	Nd	570
B	1-Chlorooctane	MV, NP, BP = 183°C	149	Nd	1552
C	2,4-Pentanedione	MV, P, BP = 133°C	100	>10 g/L[12]	785
C	Azobenzene	Dye,	182	Nd	921
C	Nonane	NV, NP, BP = 151°C	128	Not soluble	624
C	Dibutyl phthalate (DBP)	NV, MP, BP = 340°C	278	<400 mg/L (25°C)[10]	533
C	Phenyl benzoate	NV, MP, BP = 299°C	198	Nd	810
C	Toluene	V, NP, BP = 110°C	92	515 ppm (20°C)[10]	704

V: volatile; NV: not volatile; MV: medium volatile; P: polar; NP: not polar; MP: medium polar; Nd: not determined.

TABLE II
Diffusion Coefficients of 2,5-Dimethoxyacetophenone (DMA) in Polymers Around the Melt Temperature

	Diffusion coefficient ($\times 10^6$ cm^2/s)												
Temperature	EVA	HDPE	LDPE	IIDPE	EP	PP	PS	PA	EVOH	PVDC	PAN	PVC	PET
100										0.003			
120										0.008			
125	5												
135												0.05	
140										0.05			
142		6	11.5	15									
142													
145	4											0.094	
150											0.007		
155												0.18	
160					5.3							0.26	
162		17		11									
162			20										
165	6											0.37	
170							0.12						
170											0.03		
170												0.5	
180					4.7							0.5	
182		30	40	12									
182													
182													
185												0.6	
190						7.2						1.5	
190						6.3	0.33		0.3		0.09		
200					6.9								
202			50										
210						8.8							
210						12			1		0.25		
222			55										
225								0.6					
230						20					1.25		
245								1.5					
250						22							
260													1
280													3
290													2.5

neously distributed in recycled PET and their concentrations are taken equal to 100 (arbitrary units).

Transfer of surrogates to the outside of the preform is impossible because of the mold walls ($h_C = 0$).

EXPERIMENTAL DETERMINATION OF DIFFUSION COEFFICIENTS AT MOLTEN STATE

Materials

A set of 13 polymers used in food packaging was chosen for this study. These polymers are presented in Table II. Polymers were polluted with a low molecular weight UV probe, 2,5-dimethoxyacetophenone (DMA), and with a high molecular weight red dye (acid orange) (both obtained from Aldrich, Strasbourg, France).

Polluted polymers

Granules of the polymer under this study were ground in liquid nitrogen to facilitate homogenous mixing with the UV probe. The powder obtained was then immersed into a methanol solution containing at least 3000 ppm of the UV probe compound, 1500 ppm of acid orange, and 1000 ppm of antioxidant to avoid thermal degradation during the diffusion experiment. After blending, this mixture was exposed to air flow overnight to remove the methanol. Drying was then achieved in a ventilated oven, at 65°C (the methanol boiling temperature), for 4 h. The dried and contaminated powder was then extruded to produce diffusion plate specimens (100–500 μm thick).

Methods

Two plates of the same polymer (100–500 μm thick, depending on the polymer intrinsic UV absorption), one polluted and one virgin, were placed in an aluminum mold facing each other on their smallest cross section (Fig. 3). The mold was sandwiched between two iron plates and heated under a slight pressure up

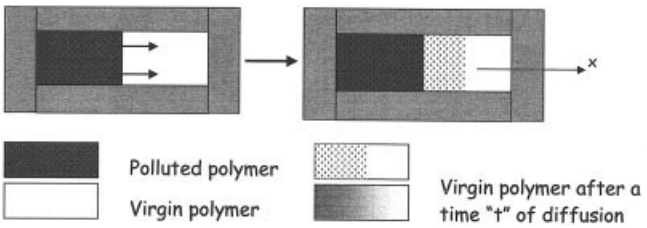

Figure 3 Principle of the diffusion test around melt temperatures.

to the testing temperature for 10 min. After this heating session, the sample was then removed and analyzed with a UV microspectrophotometer (Carl Zeiss UV–visible spectrophotometer equipped with a Xenon lamp and a microscope unit for analysis of small areas). The concentration gradient of DMA along the *x*-axis is recorded (maximum absorption at 330 nm); the diffusion coefficient is then calculated from the fit of the experimental and calculated concentration profiles, assuming Fickian diffusion and a constant diffusion coefficient (Fig. 4).

The red dye allows us to locate the initial interface between the two plates; the analysis can be done only on the initially virgin side (uncolored).

The main difficulty of the test is how to avoid blending of the two plates during their melting. This would lead to concentration gradients of DMA not connected to its diffusion. Blending of the plates is easily detected by a red color gradient, because the high molecular weight acid orange can be considered as immobile on the test time scale; therefore, any presence of a gradient is due to blending of the molten polymers.

The following precautions were used to avoid blending: the virgin and the polluted plates must have the same thickness; sample thickness must be very close to and lower than that of the mold; and the area of both plates must be slightly lower than the mold area (to compensate for the thermal expansion during melting).

Despite these precautions, at least 50% of the prepared samples cannot be used for analysis, due to blending.

EXPERIMENTAL EVALUATION OF THE POLLUTION OF BARRIER LAYER IN PREFORMS

List of surrogates

Model substances (surrogates) were selected to cover a broad range of different chemical structures, functional groups, and molecular weight (Table I). The model substances were subdivided into three groups (A, B, and C) to minimize the reactivity between them and to avoid overloading in the PET (Table I). These surrogates were incorporated into PET flakes by using dichloromethane as carrying solvent, as reported elsewhere.[14,15] The concentrations of the surrogates in PET after processing bottles were adjusted as far as possible in the range of 500-1500 ppm of each in the recycled layer (Table I) to have measurable amounts for diffusion and migration experiments.

Manufacture of preform

Impregnated PET was dried at 150°C for the first 3 h of the cycle to remove dichloromethane and for a second cycle to remove water just before injection took place. Trilayer preforms were manufactured by Amcor PET Packaging Recycling France (Dunkerque, France), the impregnated PET being used instead of the recycled PET in the usual process (Fig. 2). The impregnated

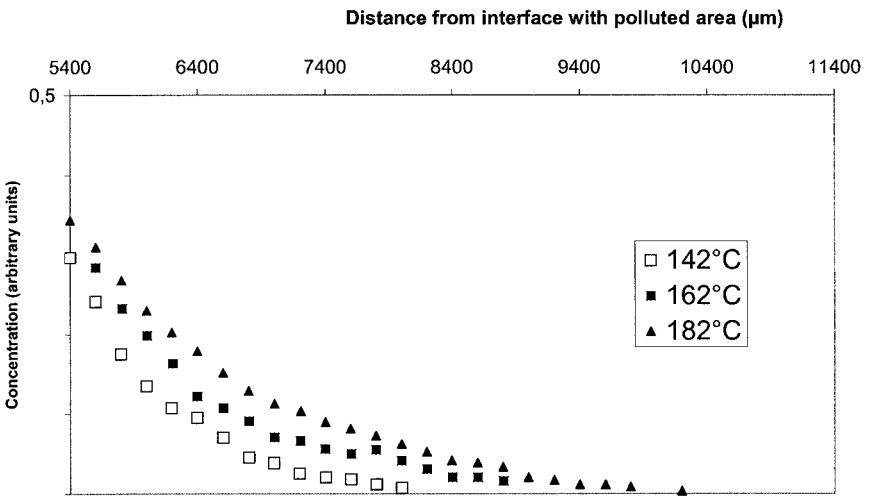

Figure 4 Diffusion profiles of DMA in HDPE at different temperatures (contact time = 10 min).

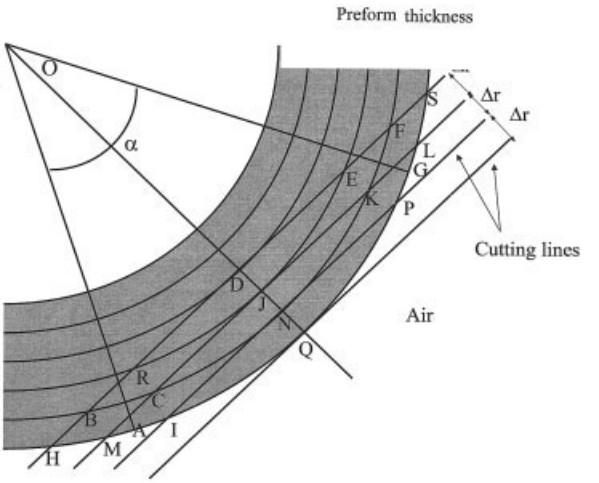

Figure 5 Top view (parallel to the direction of the microtome) of slices (thickness Δr) sectioned in the preform. O is the center of the cylindrical part of the preform; other letters represent intersections between linear cutting lines and circles delimiting rings (thickness Δr).

PET represents 25% of the preform (excluding the neck and the bottom).

Three different preform batches were processed, each containing a different group of surrogates (sets A, B, or C, Table I). Because groups B and C of surrogates contained a dye, the impregnated layer could be located visually.

Microtome sectioning of preforms and analysis of slices

The bottom cylindrical part of the preform was selected for analyses, as it is the closest to the injection point and the hottest part containing surrogates. It was cut into 1-cm-high rings (internal and external diameters were 0.8895 and 1.3210 cm, respectively). The thickness of the ring was then cut into longitudinal slices (every $\Delta r = 50$ μm), in a direction parallel to the symmetry axis of the preform (Fig. 5), using a microtome (LEICA RM 2165 microtome, 1.5 cm/min).

Slices were weighed on a microbalance (SARTORIUS M2P), and their weight was compared with the theoretical values to check their regularity. Each slice was then extracted separately for 12 h in a 100-μL vial with 50 μL dichloromethane containing an internal standard.

Quantification of surrogates in extracts

Surrogates in extracts are quantified with 2 μL injected in GC-flame ionization detector (FID) with splitless injection technique (Fisons Instrument GC 8160). Injector temperature is 250°C. Splitless time was 15 s and flow was 20 mL/min. The column was a DB5-MS J&W Scientific (15 m $\times$ 0.32 mm $\times$ 1 μm). Carrier gas (He) flow was 2 mL/min at 40°C. FID temperature was 320°C; H_2 and air flows were 25 and 250 mL/min, respectively.

Oven program for surrogates in group A was 40°C for 4 min, ramp 15°C/min to 132°C, isotherm for 6 min, heating 15°C/min until 270°C, and isotherm for 3 min.

Oven program for surrogates group B was 40°C for 4 min, ramp 10°C/min to 145°C, ramp 15°C/min to 200°C, 30 to 320°C, and isotherm for 13 min.

Oven program for surrogates group C was 40°C for 8 min, ramp 15°C/min to 170°C, ramp 2°C/min to 180°C, ramp 15 to 240°C, and isotherm for 2 min.

Mathematical treatment of extracts

Because of the cylindrical geometry of preforms, and because of the geometry of the sections (rectangular), the concentration profile of the surrogates in cylindrical layers must be reconstructed from data in rectangular samples. The procedure is schematized by Figure 5.

The weight of each slice, and the amount of surrogates, had to be mathematically corrected. Because the thickness of the ring is relatively constant, the polymer weight is then correlated with the sectioned surface. The surface areas of slices (A) were calculated by the difference of arc segments by the following equation, which is obvious from Figure 5 (example of the arc segment AQG):

$$A_{(AQG)} = \frac{1}{2}(OQ)^2(\alpha_{AOG} - \sin\alpha_{AOG}) \qquad (7)$$

where (OQ) is the radius, α is the angle (radians), and $A_{(AQG)}$ is the corresponding area.

The concentration in the first slice is directly associated with the surface (IPQ). In the second slice, the amount of surrogates is associated with the surface (MLPI). The concentration in the surface (CKN) is then deduced by subtracting the total amount of surrogates in slice 2 from those in slices (MCNI) and (KLPN), which have the same concentration as in the surface (IPQ).

In the third slice, the amount of surrogates is related to the surface (HSLM). The concentration in the surface (REJ) is obtained by subtracting from the total amount of surrogates in slice 3 from those of the surfaces, where (BRJC) and (EFKJ) are the concentration of the second surface (CKN), and (HBCM) and (FSLK) are the concentration of the first surface (IPQ).

The concentrations are calculated step by step, by recursive treatment from the outside to the inside of the ring with the increment Δr.

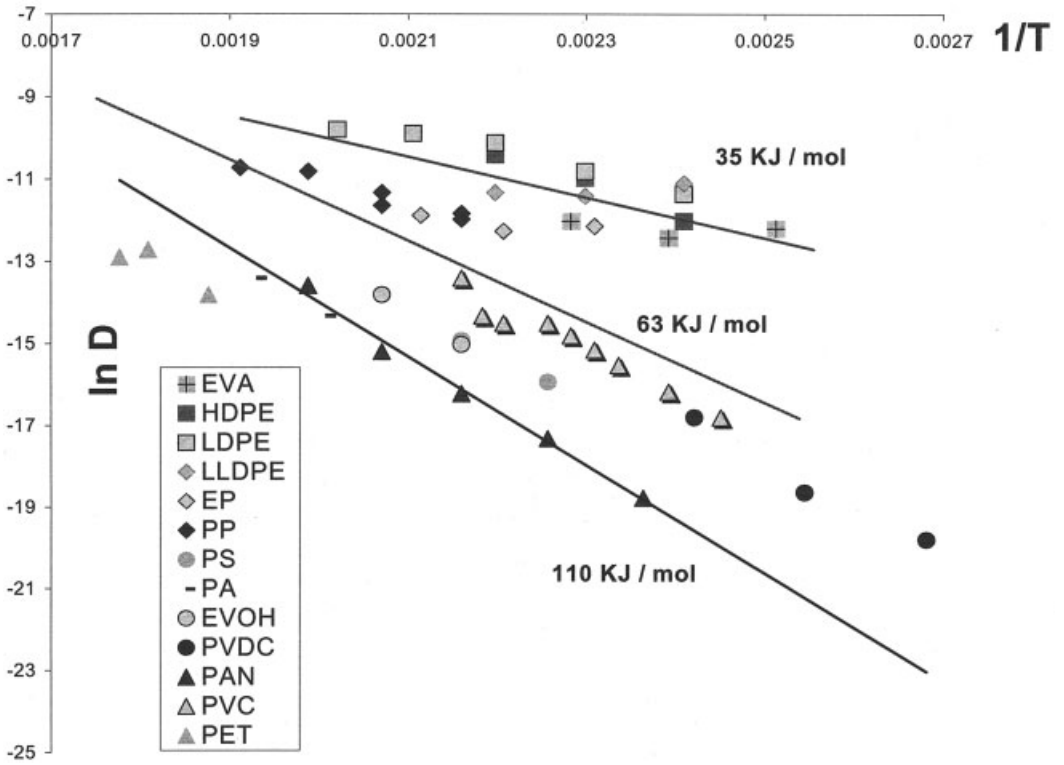

Figure 6 Arrhenius plot of DMA diffusion coefficients in different polymers at temperatures above the melt.

RESULTS AND DISCUSSION

Experimental measurement of diffusion coefficients in usual packaging polymers at molten state (fig. 6)

To measure diffusion coefficients around the melt temperature, a special test was designed: two rectangular plates were put in contact along their smallest cross section. Both plates were made of the same polymer, but one contained in addition DMA, as a UV absorbing surrogate, and acid orange (to check for possible blending of surrogates). Concentration profiles of DMA into the virgin plate, monitored by UV microscopy, allowed calculating diffusion coefficients (Table II). Diffusion coefficients obtained for polyolefins are very high and close to the values in liquids.[16] Diffusion coefficients are much lower for more polar polymers. Low values obtained for polyamide (PA-6) and for EVOH, especially, which can be linked to the formation of polar interactions, such as hydrogen bonds between the polymer containing NH or OH groups and the carbonyl groups of DMA, which lowers the mobility.[17] However, intramolecular interactions between macromolecules themselves would lead to the same effect (decrease of the network mobility, leading to a decrease of the probe mobility). Whatever the effect is, these polymers appear to keep barrier properties even in their molten state.

Effect of temperature

The range of temperatures used in the industry for processing polymers may be very large. Several temperatures were therefore tested for each polymer: the lowest temperature is the melting temperature for semicrystalline polymers, or the glass transition for amorphous polymers. Higher temperatures were chosen to cover the limits of classical processing conditions.

A low-temperature effect on the diffusion coefficient of DMA is observed in polyolefins. The most important variation is observed for high-density polyethylene (HDPE) and linear low-density polyethylene (LLDPE) (60 kJ/mol, assuming an Arrhenius-type behavior). The activation energy is lower for the other polyolefins. Therefore, an average value of 35 KJ/mol can be given for the tested polyolefin panel in the temperature range used in this study.

Effect of polymer polarity

For polar polymers, the activation energy is higher: 110 and 95 kJ/mol, respectively, for PAN and PVDC, respectively. For these polymers, diffusion in the molten state is a more thermally activated process.

It appears that the higher the diffusion coefficient of DMA, the lower its activation energy is. This trend was also observed for the diffusion of different molecules in polypropylene.[18]

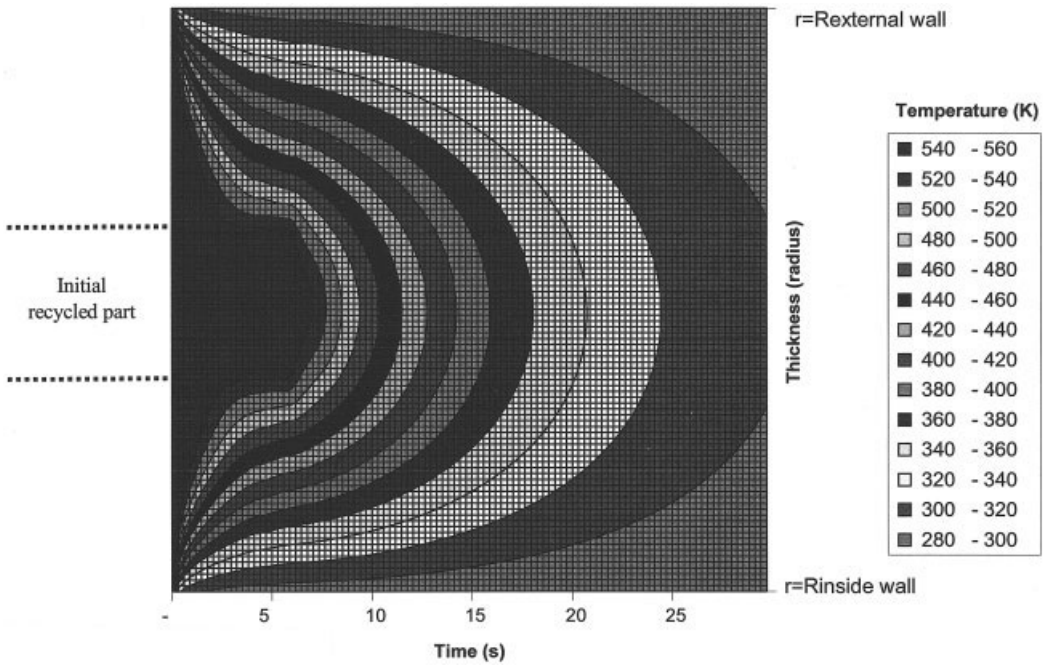

Figure 7 Simulation of temperatures profiles across PET trilayer preform, as a function of time and thickness, with $h_T = +\infty$.

In summary, the diffusion coefficient at molten state strongly depends on the polymer polarity, with polymer–polymer and/or polymer–probe (surrogate) interactions, and is more activated when the diffusion coefficient is lower. As a consequence, the materials are good barriers because of a low D and a high E_A (diffusion quickly slowed by cooling).

In the further simulations in this article, we will use as reference unrealistic (worst case) couples of (E_A, D_0) values corresponding to higher diffusion coefficients than the values obtained for DMA in PET (i.e., at 280°C: $D = 3 \times 10^{-6}$ cm^2/s and $E_A = 110$ KJ/mol) and the values obtained for DMA in any melted polymer (i.e., generally D less than 10^{-5} cm^2/s and E_A more than 35 KJ/mol around melt temperature).

Numerical simulation of diffusion profiles in PET preforms during processing

This section describes the simulations of functional barrier contamination during processing. The mold is kept at 8°C, and PET is injected at 280°C. The temperature gradient in the thickness is first calculated. Next, the diffusion of surrogates is calculated taking into account the time- and space-dependent temperature gradient.

Simulation of temperature gradient

The simulation of preform cooling is presented in Figures 7 and 8 for $h_T = +\infty$ and $h_T = 0.0074$, respectively. At $t = 4.3$ s, impregnated PET is injected for 1.5 s and then cooled. The temperature decreases quickly near the surfaces of the mold. The middle of the preform remains at 280°C for a few seconds after the end of injection and then decreases rapidly.

For $h_T = +\infty$, after 16 s, the temperature is below 100°C, even in the bulk.

Obviously if heat convection at the surface is rate-limiting, the preform cooling will be very slow; this temperature profile can be considered as a real case situation, in contact with a mold: the $h_T = 0.0074$ value was calculated from the measurements of the preform surface temperatures (by an infrared camera), immediately after removal from the mold, and after different times of cooling.

An asymmetry of temperature profiles is found, due to the cylindrical geometry, as the polymer quantity is higher near the external surface.

Simulation of surrogate diffusion in exaggerated conditions

Figure 9 shows the behavior of pollutants defined by the following unrealistic set of constants:

$$E_A = 5 \text{ KJ mol}^{-1}$$

$D_0 = 5 \times 10^{-4}$ cm^2/s (which is equivalent to $D = 1.7 \times 10^{-4}$cm^2/s at 280°C)

The concentration of surrogates is 0 all over the mold for $t < 4.3$ s. After injection of polluted PET, the diffusion of surrogates starts and continues until the end of the cooling. In this example, when D is very high, the surfaces are highly contaminated at the end

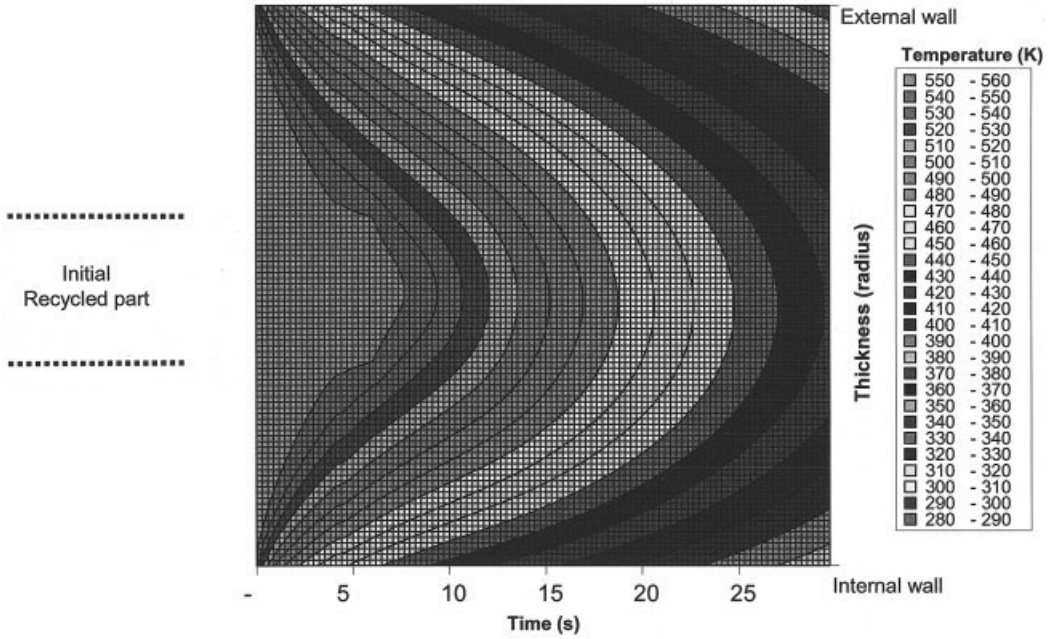

Figure 8 Simulation of temperature profiles across PET trilayer preform, as a function of time and thickness, with $h_T = +0.0074$.

of the simulation. Moreover, as the activation energy is very low, diffusion still occurs after 30 s.

As could be expected from the asymmetric temperature profiles, asymmetric concentration profiles are obtained. This asymmetry is more and more prominent as time increases, as shown by surface (external and internal) kinetics (Fig. 10).

The set of unrealistic values was chosen to illustrate the phenomenon. However, for more realistic D_0 and E_A sets of values, the contamination of the barrier layer becomes very low. This is illustrated by Figure 11. The pollution of the internal surface is simulated 30 s after injection, as a function of D_0 and E_A. The time $t = 30$ s was chosen, because when $E_A > 15$ KJ/mol, diffusion reaches a pseudoequilibrium before 30 s. Lower values of E_A are meaningless for PET.

A sharp concentration increase is observed, showing that some couples of values lead to a close to zero contamination, and some couples lead to a high contamination level. Assuming an arbitrary limit of 10^{-7}

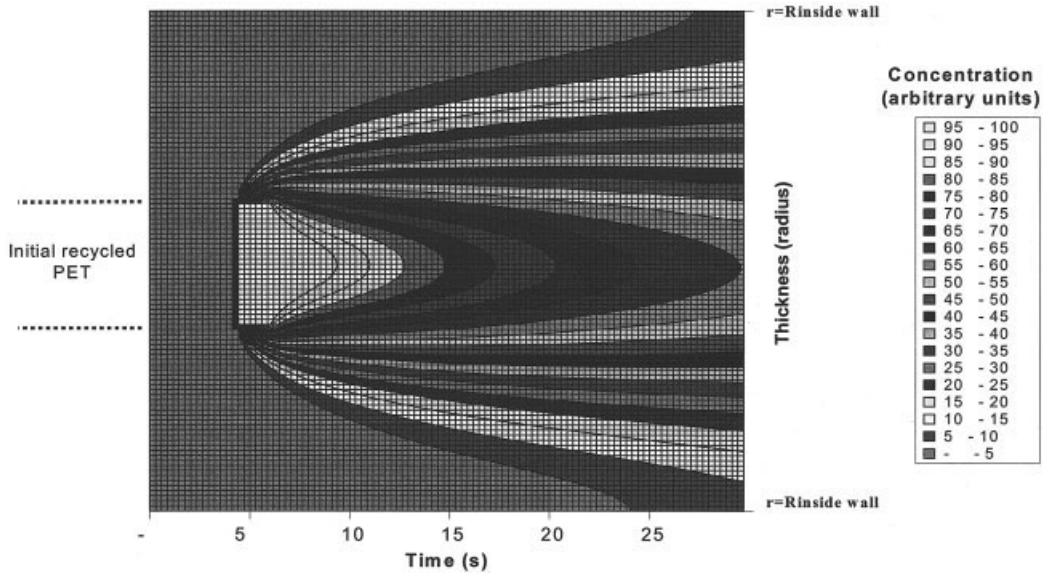

Figure 9 Simulation of concentration profiles during diffusion of a surrogate in the thickness of a preform, as a function of time and of thickness (calculated with $h_T = 0.0074$, $E_A = 5$ KJ mol^{-1}, and $D_0 = 5 \times 10^{-4}$ cm^2/s).

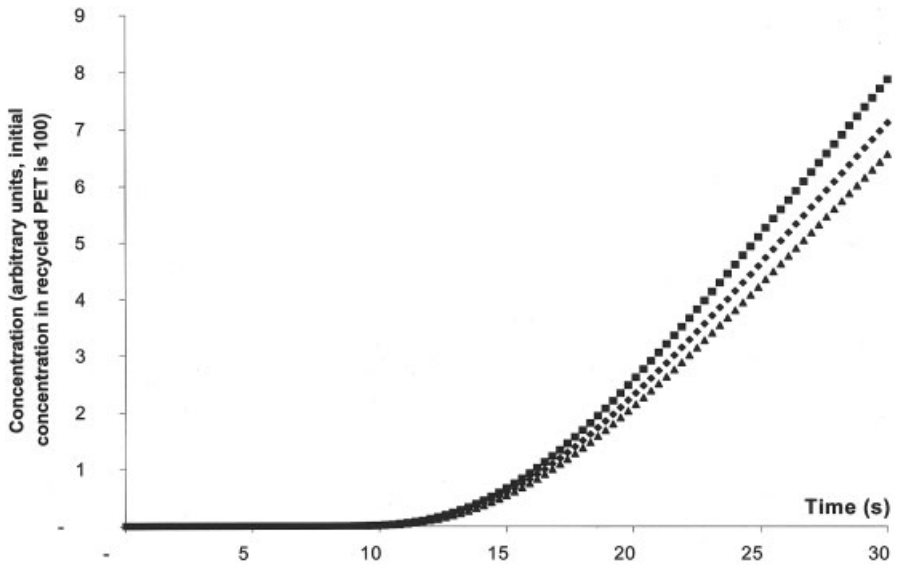

Figure 10 Concentrations at surfaces of a preform obtained by simulation with $h_T = 0.0074$, $E_A = 5$ KJ/mol, and $D_0 = 5 \times 10^{-4}$ cm^2/s. Comparison between inside (■) and outside (▲) concentrations in a cylindrical preform, and on surface plane sheet (♦) in the same conditions.

for the surface contamination (very low; this has to be compared to $C_0 = 100$), we can look in the plane ($C_{ext} = 10^{-7}$) for which (D_0, E_A) couples the surface is contaminated. Isodiffusion coefficient straight lines are represented in the plane. The ($D_{280°C} = 10^{-5}$ cm^2/s) straight line has no intersection (in the studied unrealistically large area) with the contamination surface map, showing that no (D_0, E_A) couple is compatible with a 10^{-7} surface contamination. Even such a low contamination level cannot be reached.

Obviously the straight lines corresponding to lower $D_{280°C}$ values give no intersection with the contamination surface map. It can be also concluded that all situations with $D_{280°C} < 10^{-5}$ cm^2/s lead to a negligible contamination of the barrier layer.

Diffusion coefficients of surrogates and of contaminants are expected to be lower than 10^{-5} cm^2/s, as is the case for data in this work (measured for PET or for those overestimated from polyolefin behavior) (Table II).

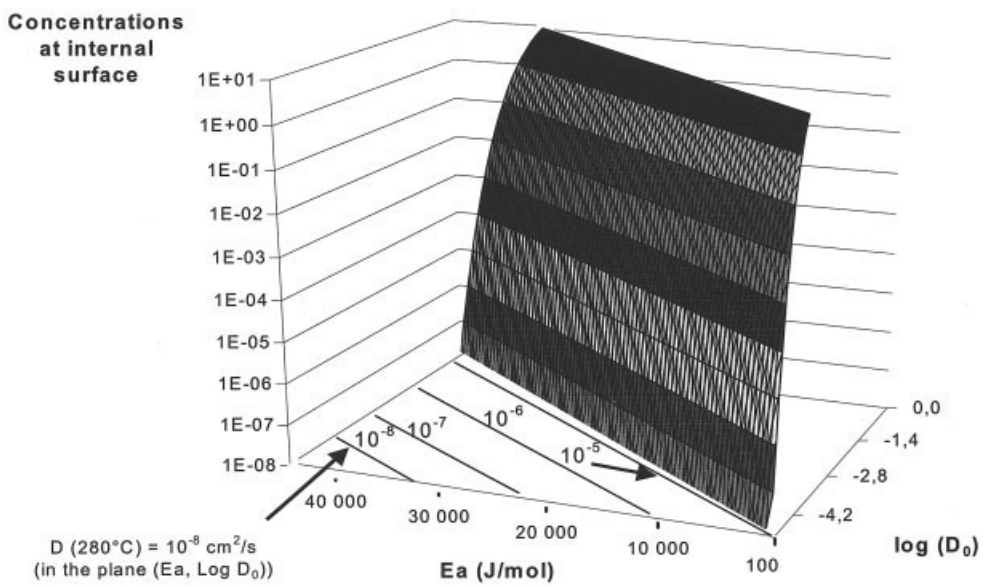

Figure 11 Concentrations at the surface of a preform after 30 s in the mold for $h_T = 0.0074$ (injection of virgin PET 4.3 s, injection of recycled 1.5 s, cooling 30 s) as a function of E_A and Log(D_0 cm^2/s). Values of E_A and Log(D_0) corresponding to $D = 10^{-5}$ cm^2/s are represented in the plane (E_a, Log D_0) by a straight line.

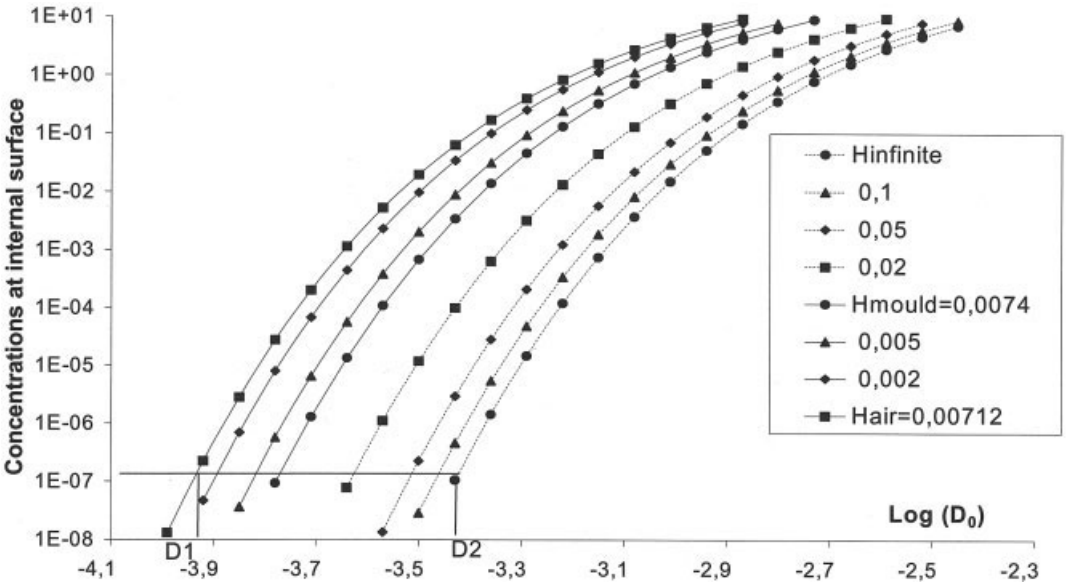

Figure 12 Concentration at the inside surface after 30 s in the mold for different h_T, as a function of Log(D_0 cm^2/s). E_A = 10 KJ/mol.

Effect of h_t

The previous simulations were made by using an h_T value, supposed to correspond to the real process studied in this work (calculated from experimental temperature measurements). As the efficiency of heat exchange can vary with the types of mold, we investigate in this section the influence of the variable h_T.

Figure 12 shows the variation of the concentration at the surface, as a function of D_0, for different values of h_T (from h_T infinite, instantaneous surface heat exchange, to h_T = 0.00712, which corresponds to exchanges with static air, i.e., worst case). A pessimistic unrealistic value is taken for E_A (E_A = 10 KJ/mol).

If we arbitrarily take a surface pollution limit of $C = C_0/10^9 = 10^{-7}$, we can deduce the highest acceptable D_0 values, corresponding to each h_T value:

for $h_T = 7.12 \times 10^{-4}$, the highest acceptable $D_0 = 1.12 \times 10^{-4}$ cm^2/s
for $h_T \rightarrow +\infty$, the highest acceptable $D_0 = 3.98 \times 10^{-4}$ cm^2/s.

This corresponds to the following range for the diffusion coefficient at 280°C: 1.3×10^{-5} to 4.5×10^{-5} cm^2/s. These values are again higher than the reference values measured is this work.

Experimental determination of concentration profiles of surrogates in the PET preform

Figure 13 shows the concentration profiles obtained with surrogate set B. The other sets (A and C) led to the same type of results, for instance,

1. All molecules have the same behavior, even if they may have very different chemical and physical characteristics. For example, Uvitex OB has the highest molecular weight, then the lowest diffusion coefficient. However, its concentration profile in the thickness is the same as that of other substances. This shows that no detectable diffusion occurs.
2. The profiles are almost vertical between polluted and virgin layers, which shows that blending and diffusion effects are limited.
3. The recycled part of the preform is not in the center of the preform total thickness (4.32 mm). According to the manufacturer, this off-center is inherent to the coinjection process and cannot be improved. As a consequence, the thickness of the functional barrier in the preform is around 0.82 mm, corresponding roughly to 20% of the total thickness. This corresponds, in the final bottle, to a 55- to 60-μm-thick functional barrier. An observation under microscopy of bottle wall slices obtained from the preforms containing dyes (Uvitex OB and azobenzene) showed that the functional barrier thickness is around 60 to 70 μm.

The (not optimal) dimension of the functional barrier is rather due to a dissymmetry of the inner layer injection, and a polymer layer blending effect, than due to diffusion of pollutants during processing.

CONCLUSION

Functional barriers must behave as barriers even in molten polymers. A double approach was used to

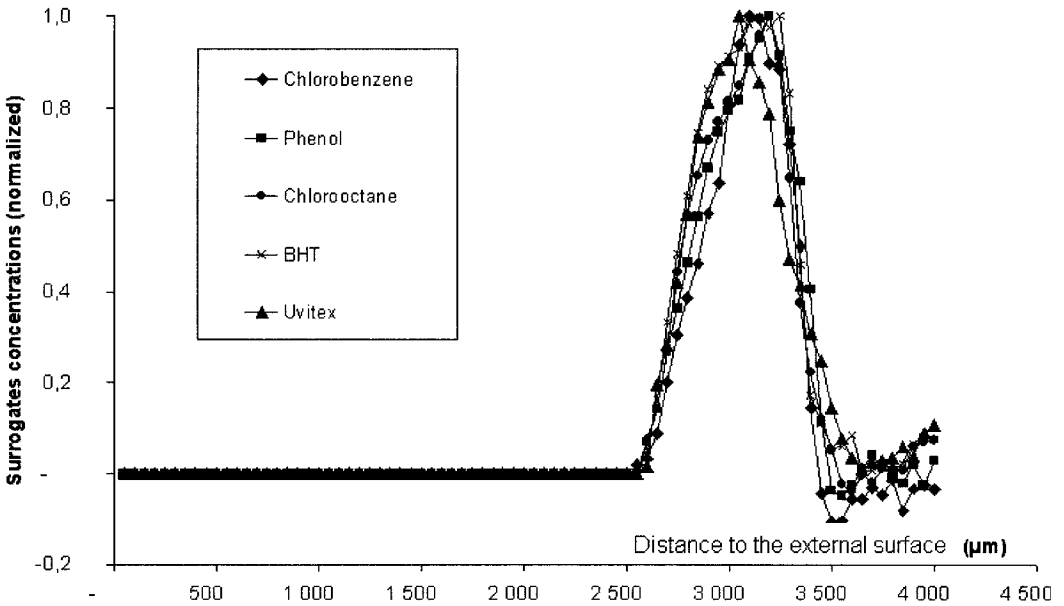

Figure 13 Experimental surrogate concentration profiles (with surrogate set B) in the thickness of a preform.

demonstrate that pollutants introduced in a preform inner layer do not diffuse into the functional barrier during processing.

In the first approach (simulation), the functional barrier pollution was simulated by numerical analysis. Unrealistic sets of diffusion parameters are necessary to obtain a sensible pollution of the virgin layer.

In the second approach (experimental), the diffusion of real pollutants is overestimated by the use of low molecular weight surrogates including nonpolar species which do not interact with PET. The radial concentration profiles of the surrogates show that no diffusion occurred for any surrogate during preform manufacturing.

Our positive conclusion with PET preforms cannot be generalized to any PET-based material. In fact, diffusion is negligible compared to the thickness of PET preforms. For thinner materials (generally the case for coextrusion), the conclusions could be less definite.

Useful surrogate diffusion data, determined in various polymers at molten state by a model test, are available in this article and can be used for numerical simulations.

The authors thank ECO-EMBALLAGES, ADEME and Region Champagne-Ardenne for grants for P.Y.P. (E-A, A, RCA) and for Y.N.G. (RCA) and for financial support. Part of this work was also supported by the EU DG Research (FAIR 984318 research program).

References

1. Bayer, F. L. Food Addit Contam 1997, 14, 661–670.
2. Franz., R.; Huber, M.; Piringer, O.; Damant, A. P.; Jickells, S. M.; Castle, L. J Agric Food Chem 1996, 44, 892–897.
3. Piringer, O.; Franz, R.; Huber, M.; Begley, T. H.; McNeal, T. P. J Agric Food Chem 1998, 46, 1532–1538.
4. Franz, R.; Huber, M.; Piringer, O. Food Addit Contam 1997, 14, 627–640.
5. Perou, A. L.; Vergnaud, J. M. Plast Rubber Compos 1999, 28 (2), 74–79.
6. Perou, A. L.; Laoubi, S.; Vergnaud, J. M. J Appl Polym Sci 1999, 73 (10), 1939–1948.
7. Reynier, A.; Dole, P.; Feigenbaum, A. Food Addit Contam 2002, 19 (1), 89–102.
8. Vergnaud, J. M. Liquid Transport Processes in Polymeric Materials. Modeling and Industrial Applications; Prentice Hall: Englewood Cliffs, NJ, 1991.
9. Morikawa, J.; Hashimoto, T. Polymer 1997, 38, 5397–5400.
10. Montgomery, J. H.; Welkom, L. M. Groundwater Chemicals Desk Reference; Lewis Publishers: Boca Raton, FL, 1991.
11. Weast, R. C.; Astle, M. J.; Beyer, W. H. CRC Handbook of Chemistry and Physics; CRC Press: Boca Raton, FL, 1986–1987.
12. Budavari, S.; O'neil, M. J.; Smith, A.; Heckelman, P. E.; Kinneary, J. F. The Merck Index, 12th ed.; Merck Research Laboratories, Division of Merck & Co.: Whitehouse, NJ, 1996.
13. CIBA, Technical data of BHT; Raschig AG, Sparte Chemie, Mundenheimer Str. 100, D-67061 Ludwigshafen.
14. Pennarun, P. Y.; Dole, P.; Feigenbaum, A.; Saillard, P. Food Addit Contam to appear.
15. Pennarun, P. Y.; Dole, P.; Feigenbaum, A. J Appl Polym Sci to appear.
16. Brandrup, J.; Immergut, E. H. Polymer Handbook, 3rd ed.; Wiley-Interscience: New York, 1989.
17. Feigenbaum, A.; Ducruet, V.; Riquet, A. M.; Scholler, D. J Chem Educ 1993, 883–886.
18. Reynier, A.; Dole, P.; Feigenbaum, A. J Appl Polym Sci 2001, 82 (10), 2434–2443.